www.elsevier.nl/locate/jorganchem
Journal of Organometallic Chemistry 592 (1999) 109–114

Linear and non-linear optical properties of arene–Fe–Cp complexes

Christoph Lambert [a,*], Wolfgang Gaschler [a], Manfred Zabel [b], Ralf Matschiner [c], Rüdiger Wortmann [c]

[a] *Institut für Organische Chemie, Universität Regensburg, Universitätsstrasse 31, D-93040 Regensburg, Germany*
[b] *Instrumentelle Analytik der Fakultät für Chemie und Pharmazie, Universität Regensburg, Universitätsstrasse 31, D-93040 Regensburg, Germany*
[c] *Fachbereich Chemie, Universität Kaiserslautern, Erwin-Schrödinger-Straße, D-67663 Kaiserslautern, Germany*

Received 14 May 1999; received in revised form 16 June 1999; accepted 29 July 1999

Abstract

Ionic [arene–Fe–Cp]$^+$ fragments were used as electron acceptors in combination with dimethylamino or pyridoneiminyl donors to form push–pull substituted chromophores. While a tolane derivative showed high second-order non-linear optical activity (measured by hyper-Rayleigh scattering), an analogous pyridoneimine derivative did not. With the help of an X-ray crystal structure analysis this discrepancy was traced back to a cyanine-like structure of the imine. Semiempirical INDO/S calculations support this conclusion. © 1999 Elsevier Science S.A. All rights reserved.

Keywords: Non-linear optics; Hyper-Rayleigh scattering; UV–vis spectroscopy; Iron; Chromophores; Palladium-catalysed cross coupling

---

1. Introduction

The electron-donating and -accepting capabilities of organoligand–metal fragments have been successfully applied to push–pull substituted chromophores in order to achieve high second-order non-linear optical (NLO) responses [1]. Ferrocene, especially, is widely used as an organometallic electron donor [2]. It combines the advantage of high stability, electrochemical activity and the fact that it is easily incorporated into larger organometallic molecules by standard synthetic procedures. The electron-donor capacity of ferrocene in terms of promoting charge transfer (CT) excitation and, associated with this CT, quadratic hyperpolarisability, has been estimated to be about that of a methoxy group [2a,b]. In contrast, the electron-acceptor counterparts of ferrocene, ionic [arene–Fe–Cp]$^+$ fragments, have not been used in organometallic NLO chromophores, although their electrochemical and photochemical properties have led to intense investigations [3].

Recently, we have focused on ammonio (R_3N^+) and phosphonio (R_3P^+) acceptor groups that polarise π-electron systems in the π-plane in order to form one-dimensional NLO-chromophores [4]. In contrast, the [Cp–Fe]$^+$ fragment might polarise π-electron systems perpendicular to the π-plane. The purpose of this paper is to elucidate the linear and non-linear optical properties of organometallic NLO chromophores where the acceptor functionality is a [benzene–Fe–Cp]$^+$ moiety being combined with a conventional electron donor via a π-electron spacer attached to the benzene ring.

2. Results and discussion

While chloroarenes are usually not susceptible to palladium-catalysed Stille couplings under normal conditions [5], the analogous [arene–Fe–Cp]$^+$ complexes readily undergo cross-coupling reactions with a dimethylamino-substituted phenylethynyltrimethylstannane (see Scheme 1), leading to the one-dimensional tolane chromophores **1** and the pentamethyl analogue **2**. The latter compound was synthesised because of its

---

* Corresponding author. Tel.: +49-941-9434373; fax: +49-941-9434984.
E-mail address: christoph.lambert@chemie.uni-regensburg.de (C. Lambert)

PII: S0022-328X(99)00497-0

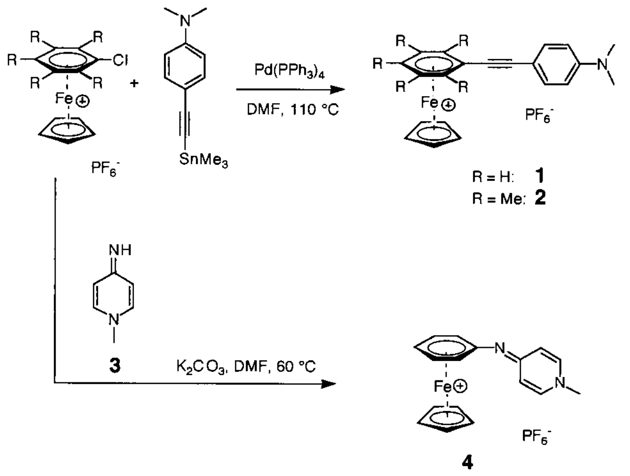

Scheme 1.

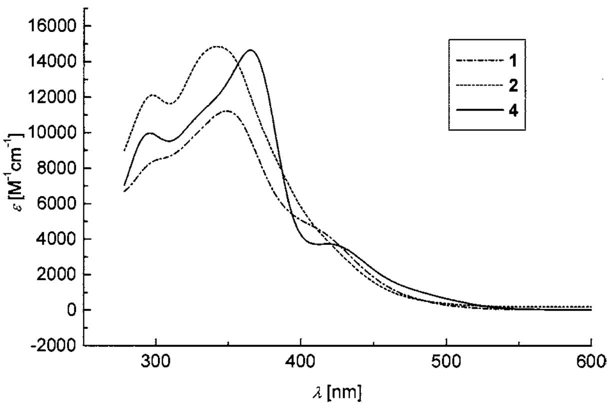

Fig. 1. UV–vis spectra of **1**, **2**, and **4** in MeCN.

higher light stability compared to **1**. In addition, [arene–Fe–Cp]$^+$ was derivatised by nucleophilic substitution with imine **3**, which yielded the pyridoneimine **4**. These reactions demonstrate the strong electron-withdrawing character of [arene–Fe–Cp]$^+$ and thus prompted us to investigate their optical properties. Derivatives **1** and **2** combine the ionic iron acceptor with the conventional dimethylamino donor, whereas the donor in **4** is the *N*-methylpyrid-4-yl group, which should act as an electron donor because it gains aromaticity upon electron loss.

Fig. 1 shows the UV–vis spectra of **1**, **2** and **4** in MeCN. All derivatives have intense bands at ca. 348 nm (**1**), 336 nm (**2**), 365 nm (**4**), which are attributed to intraligand CT excitations. At longer wavelengths, there are weaker MLCT bands at ca. 400–420 nm and at shorter wavelengths there are LMCT or MLCT bands at ca. 300 nm [6]. From deconvolutions of the spectra with Gaussian curves we estimate the band width at half-height of the intraligand CT bands to be ca. 5700 cm^{-1} for **1**, ca. 5400 cm^{-1} for **2**, and to be distinctly smaller (ca. 2900 cm^{-1}) for **4**. While the CT bands of **1** and of **2** are weakly solvatochromic (**1**: 352 nm in THF; **2**: 344 nm in THF) that of **4** is not (365 nm in THF).

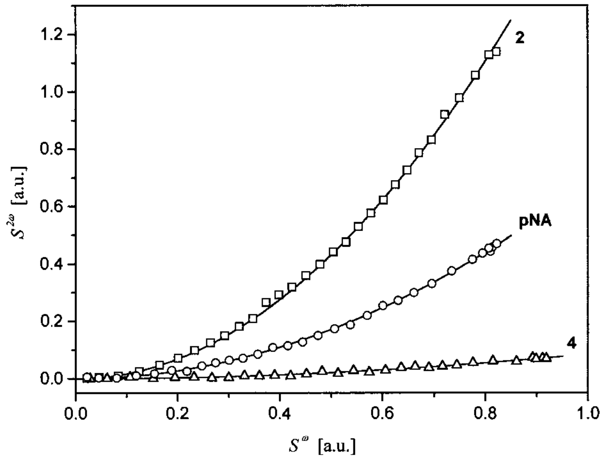

Fig. 2. HRS signal $S^{2\omega}$ as a function of the fundamental laser intensity S^{ω} for acetonitrile solutions of compound **2** (c = 9.18 mol m^{-3}), **4** (c = 15.71 mol m^{-3}) and the calibration standard pNA (c = 16.12 mol m^{-3}). Each point represents an average over 300 laser pulses. The solid lines are quadratic fits.

The quadratic hyperpolarisability β of **2** and of **4** were determined by hyper-Rayleigh scattering (HRS) in MeCN at 1064 nm fundamental energy [7]. The HRS experiments were carried out as described with all details in ref. [7b]. The experimentally detected HRS signal $S^{2\omega}$ is a quadratic function of the incident intensity S^{ω}. Typical results are shown in Fig. 2 for derivatives **2** and **4** as well as for the reference standard *para*nitroaniline (pNA). Such curves were taken and fitted for several different concentrations. The β values were finally calculated from the slopes of linear regression of the quadratic fit coefficients versus the concentration of the solutes. pNA was used as a reference compound $\{\beta^{1064} = 49.6 \times 10^{-50}$ cm^3 V^{-2} (134×10^{-30} esu) in MeCN, β^{T} convention used [7b, 8]$\}$. Measurements of **1** were hampered due to the increased light sensitivity of **1** versus **2**. The hexamethyl derivative **2** was stable under the conditions of the HRS experiment. The β value of **2** is 120×10^{-50} cm^3 V^{-2} (318×10^{-30} esu) and the static value is 60×10^{-50} cm^3 V^{-2} (168×10^{-30} esu) (static values calculated by extrapolation via two-level model). This value is about that of 4-dimethylamino-4′-cyanotolane whose static β value is 66×10^{-50} Cm^3 V^{-2} (174×10^{-30} esu, $\lambda_{max} = 373$ nm in CHCl$_3$) [9]. In contrast, imine **4** showed no measurable SHG signal. This behaviour deserves an explanation, as the CT bands of **2** and of **4** are at similar energy and have almost equal intensity.

The difference in hyperpolarisability of **2** and **4** might be attributed to an unfavourable electronic structure of **4** which expresses itself in a small bond length alternation (BLA) in the conjugation path. It is known from

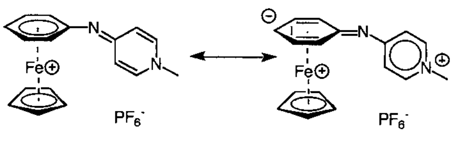

4

Scheme 2.

Table 1
Selected bond distances (Å) of **4** [a]

N1–C6	1.368(3)	C8–C9	1.400(4)
N1–C12	1.327(3)	C9–C10	1.402(4)
N2–C14	1.350(3)	C10–C11	1.409(3)
N2–C15	1.353(3)	C12–C13	1.422(3)
N2–C17	1.461(3)	C12–C16	1.429(3)
C6–C7	1.417(3)	C13–C14	1.355(3)
C6–C11	1.426(3)	C15–C16	1.352(3)
C7–C8	1.407(4)		

[a] Angle C12–N1–C6 = 124.7(2)°, angle between the phenyl ring and the pyridinium ring = 43.2°.

the studies of Marder and co-workers that the BLA can be used as an indicator for favourable electronic structure: e.g. for many olefins the optimal BLA at which β displays a maximum is ca. 5 pm [10]. In cases where the BLA is small or zero, the difference between excited- and ground-state dipole moment vanishes (cyanine limit) and, as can be seen by the two-level equation (Eq. (1), where μ_{01} is the transition moment, $\Delta\mu$ is the dipole moment difference between ground and excited state and ω_{01} is the CT transition energy), β approaches zero. It is clear from the strong C≡C triple bond force constants that the tolane in **2** will not experience strong alternation in bond lengths upon changing the donor or acceptor functionalities. This is completely different in **4**, where two mesomeric structures might equally contribute to the electronic situation: one with a chinoid pyridyl and a benzoid phenyl ring, the other with the benzoid and chinoid structures exchanged (see Scheme 2). A single-crystal X-ray analysis of **4** revealed that the pyridyl moiety has a chinoide distortion compared to pyridinium structures (see Fig. 3 and Table 1). The C12–N1 bond (1.33 Å) is ca. 5 pm longer and the C6–N1 bond (1.37 Å) is ca. 5 pm shorter than in aromatic Schiff bases [11]. The BLA in the imine bridge thus is ca. 4 pm. Together with the distinctly smaller band width at half-height, these features indicate a cyanine-like structure with a too small BLA and a negligible β value. It must be stressed that while symmetrical cyanines show a zero BLA, this does not necessarily hold true for unsymmetrical donor–acceptor systems where the dipole moment difference is zero at a BLA ≠ 0, although this value might be quite small [12].

$$\beta_{zzz} = \frac{6\mu_{01}^2 \cdot \Delta\mu}{\hbar^2\omega_{01}^2} \qquad (1)$$

Our interpretation is supported by semiempirical INDO/S calculations (Table 2) [13]. The CIS was based on ten occupied and ten virtual orbitals resulting in a CI matrix with 100 microstates. The calculated results from the CI computations as well as the static β values calculated by a sum-over-states method are given in Table 2 and are in reasonable agreement with the experiment. While the CT bands between ligands and the metal centre are generally weak, the CI calculations revealed strong intraligand CT excitations (LCT) at 341 nm (**2**) and 349 nm (**4**) in good agreement with the experiment. However, the dipole moment difference associated with the LCT excitation is large (44.0×10^{-30} C m, 13.2 D) for **2** but rather small (4.0×10^{-30} C m, 1.2 D) for **4**. Using the two-level approximation (Eq. (1)), this explains the high β_{zzz} value for **2** and the

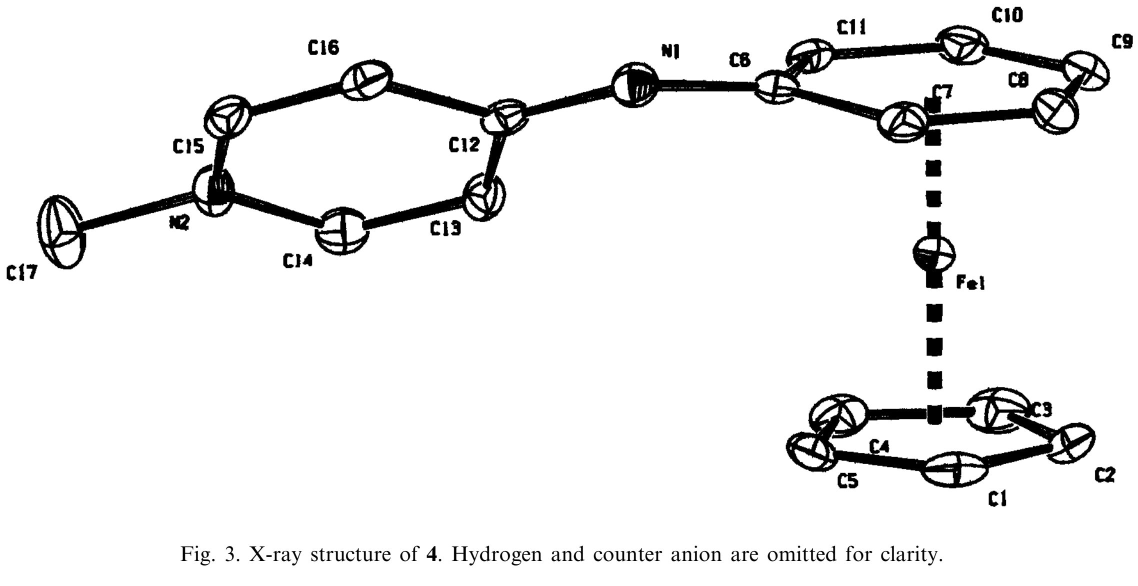

Fig. 3. X-ray structure of **4**. Hydrogen and counter anion are omitted for clarity.

Table 2
INDO/S calculated optical properties of **2** and **4**

	λ_{max} (nm)	f	Band type	$\Delta\mu$ (10^{-30} C m) (D)	β^0 (10^{-50} cm^3 V^{-2}) (10^{-30} esu)
2	374	0.012	MLCT	2.7 (0.8)	
	341	0.986	LCT	44.0 (13.2)	38 (102) [a]
	317	0.023	LMCT	16.7 (5.0)	
4	367	0.015	MLCT	2.7 (0.8)	
	349	0.722	LCT	4.0 (1.2)	<7.2 (20) [b]
	329	0.022	MLCT	20.4 (6.1)	

[a] β_{zzz}.

[b] All tensor components are smaller.

absence of any measurable SHG signal for **4** in accordance with the calculations (see Table 2). In addition, the INDO/S calculations suggest that in **2** the only CT excitation contributing to β is that within the tolane system; the MLCT excitation at longer wavelength and the LMCT at shorter wavelength are polarised perpendicular to the tolane (zzz) axis and no other β tensor component besides β_{zzz} is significant in **2**.

3. Conclusions

[Arene–Fe–Cp]$^+$ substituents are effective acceptor units that can be used in push–pull substituted π-electron systems for non-linear optics. The quadratic hyperpolarisability of **2** is comparable to that of e.g. 4-dimethylamino-4′-cyanotolane at somewhat shorter CT absorption wavelength. In this respect, one can conclude that the electron-acceptor strength of a [arene–Fe–Cp]$^+$ moiety is about that of a 4-cyanophenyl group. A major drawback of the compounds studied are MLCT bands at longer wavelengths than the intraligand CT band. These MLCT bands do not contribute to the hyperpolarisability and limit the blue transparency as is often observed for organometallic derivatives [1]. One possible way to improve the efficiency–transparency trade-off is to use more extended π-systems with LCT bands at similar or lower energy than the MLCT bands and which then display intrinsically higher optical non-linearities. Although this will improve the non-linearity only because of the red shift of the intraligand CT, there is at least no loss of transparency due to ineffective MLCT bands.

4. Experimental

4.1. *η^6-Chloropentamethylbenzene-η^5-cyclopentadienyl-iron-(II)-hexafluorophosphate*

Chloropentamethybenzene [14] (6.8 g, 37 mmol), ferrocene (14.9 g, 80 mmol), aluminium powder (1.0 g, 37 mmol) and aluminiumchloride (20.0 g, 150 mmol) were stirred under a nitrogen atmosphere at 120°C for 14 h. The melt was cooled and hydrolysed gently with ice. The resulting suspension was filtered, the filtrate was washed with petrol ether and the product was precipitated by adding an NH_4PF_6 solution (7 g in 50 ml of water) to the aqueous phase. The crude product was filtered off, dissolved in acetone, dried over Na_2SO_4 and precipitated by adding diethyl ether. Yield 7.20 g (43%) of a yellow powder; m.p. (dec.) 200°C; ^{1}H-NMR (250 MHz, acetone-d_6): $\delta = 4.95$ (s, 5 H, Cp), 2.78 (s, 6 H, *o*-CH_3), 2.67 (s, 6 H, *m*-CH_3), 2.60 (s, 3 H, *p*-CH_3); ^{13}C-NMR (62.9 MHz, acetone-d_6): $\delta = 108.7$, 100.9, 100.5, 99.3, 81.0, 18.6, 17.8, 17.5; MS (PI-FD, acetone-d_6) m/z: 303 (cation$^+$); $C_{16}H_{20}ClF_6FeP$ (448.6), Anal. Calc. C 42.84, H 4.49, found C 42.61, H 4.31%.

4.2. *η^6-[4-(N,N-Dimethylamino)phenylethynyl-benzene]-η^5-cyclopentadienyl-iron-(II)-hexafluorophosphate (**1**)*

η^6-Chlorobenzene-η^5-cyclopentadienyl-iron-(II)-hexafluorophosphate [15] (404 mg, 0.90 mmol), [4-(*N*,*N*-dimethylamino)phenylethynyltributylstannane (prepared by the reaction of lithio-4-(*N*,*N*-dimethylamino)phenylacetylene with chlorotributylstannane in Et_2O at −78°C) (677 mg, 1.58 mmol) and $Pd(PPh_3)_4$ (78 mg, 0.068 mmol) were dissolved in 5 ml of dry DMF under nitrogen atmosphere. This solution is stirred at 110°C for 2.5 h under exclusion of light. The solvent was removed in vacuo and the resulting dark oil was washed with petrol ether. The residue was dissolved in acetone and precipitated with a large excess of diethyl ether. The crude product was again dissolved in acetone, filtered over neutral alumina and precipitated with diethyl ether. Yield 340 mg (78%) of a yellow powder; m.p. (dec.) 202°C; IR (KBr) 2212 cm^{-1}; ^{1}H-NMR (250 MHz, acetone-d_6): $\delta = 7.48$ (m, AA′, 2 H), 6.78 (m, BB′, 2 H), 6.59 (5 H, phenyl), 5.29 (s, 5 H, Cp), 3.05 (s, 6 H, NMe_2); ^{13}C-NMR (62.9 MHz, acetone-d_6): $\delta = 152.4$, 134.3, 112.6, 107.7, 96.0, 90.1, 89.9, 89.2, 87.7, 83.5, 79.2, 40.0; MS (PI-FD, MeOH) m/z:

342 (cation$^+$); $C_{21}H_{20}F_6FeNP$ (487.2), Anal. Calc. C 51.77, H 4.14, N 2.87, found C 51.71, H 4.32, N 3.03%.

4.3. *η^6-[4-(N,N-Dimethylamino)phenylethynyl-pentamethylbenzene]-η^5-cyclopentadienyl-iron-(II)-hexafluorophosphate* (**2**)

η^6-Chloropentamethylbenzene-η^5-cyclopentadienyl-iron-(II)-hexafluorophosphate (717 mg, 1.60 mmol), [4-(*N*,*N*-dimethylamino)phenylethynyltributylstannane (814 mg, 1.90 mmol) and $Pd(PPh_3)_4$ (100 mg, 0.087 mmol) were dissolved in 5 ml of dry DMF under nitrogen atmosphere. This solution was stirred at 110°C for 3 h under exclusion of light. The solvent was removed in vacuo and the resulting dark oil was washed with petrol ether. The residue was dissolved in acetone and precipitated by a large excess of diethyl ether. The crude product was purified by column chromatography on neutral alumina first with CH_2Cl_2 and then with $CH_2Cl_2 + 5\%$ acetone. The product was precipitated from concentrated solutions with diethyl ether. Yield 260 mg, (29%) of a yellow powder; m.p. (dec.) 258–260°C; IR (KBr) 2203 cm^{-1}; ^{1}H-NMR (250 MHz, acetone-d_6): $\delta = 7.54$ (m, AA′, 2 H), 6.80 (m, BB′, 2 H), 4.87 (s, 5 H, Cp), 3.06 (s, 6 H, CH_3), 3.05 (s, 6 H, NMe_2), 2.63 (s, 6 H, CH_3), 2.60 (s, 3 H, CH_3); ^{13}C-NMR (62.9 MHz, acetone-d_6): $\delta = 152.3$, 134.0, 112.7, 108.3, 101.5, 100.1, 100.0, 99.9, 88.4, 83.4, 80.4, 40.1, 19.4, 17.3, 17.3; MS (PI-FD, CH_2Cl_2) m/z: 412 (cation$^+$); $C_{26}H_{30}F_6FeNP$ (557.4), Anal. Calc. C 56.03, H 5.43, N 2.51, found C 55.75, H 5.44, N 2.43%.

4.4. *η^6-[(N-Methyl-4-pyridoneiminyl)benzene]-η^5-cyclopentadienyl-iron-(II)-hexafluorophosphate* (**4**)

N-Methyl-4-pyridoneimine [16] (6.2 g, 5.7 mmol), η^6-chlorobenzene-η^5-cyclopentadienyl-iron-(II)-hexafluorophosphate (1.9 g, 5.0 mmol) and K_2CO_3 (2.8 g) were dissolved in 10 ml of DMF and stirred at 60°C for 14 h. Water (100 ml) was added and the mixture extracted with CH_2Cl_2. The solvents were removed in vacuo; the residue was purified by column chromatography on neutral alumina first with acetone–water (4:1) and then with acetone–water (1:1). The eluents were concentrated and extracted with CH_2Cl_2. The product was precipitated by adding diethyl ether. Yield 600 mg (27%) of an orange powder, m.p. (dec.) 200–201°C; IR (KBr) 1650 cm^{-1}; ^{1}H-NMR (250 MHz, acetone-d_6): $\delta = 7.56$ (m, AA′, 2 H), 6.53 (m, BB′, 2 H), 6.17 (5 H, phenyl), 5.00 (s, 5 H, Cp), 3.76 (s, 6 H, NMe); ^{13}C-NMR (62.9 MHz, acetone-d_6): $\delta = 161.0$, 141.5, 128.9, 113.1, 87.9, 83.1, 80.1, 77.1, 43.6; MS (PI-FD, CH_2Cl_2) m/z: 305 (cation$^+$); $C_{17}H_{17}F_6FeN_2P$ (450.2), Anal. Calc. C 45.36, H 3.81, N 6.22, found C 45.41, H 3.99, N 6.22%.

4.5. *X-ray crystallographic data of* **4**

$C_{17}H_{17}F_6FeN_2P$, $M = 450.2$. Data were collected on a STOE-Imaging Plate System with monochromatic Mo–K$_\alpha$ radiation ($\lambda = 0.71069$ Å); $T = 120(2)$ K; monoclinic, space group $P2_1/c$; $a = 7.3316(6)$ Å, $b = 14.1435(9)$ Å, $\beta = 99.809(9)°$, $c = 16.7866(14)$ Å; $V = 1715.2(2)$ Å^3; $Z = 4$; $\rho_{calc.} = 1.743$ g cm^{-3}; red plates ($0.12 \times 0.20 \times 0.44$ mm^3); scan range $1.89 < \theta < 25.61°$; 11 492 collected, 3155 independent and 2247 observed ($I > 2\sigma(I)$) reflections; the structure was solved with direct methods (SHELXS-93) and refined against F^2. All non-hydrogen atoms were refined anisotropically, the hydrogen atoms isotropically in fixed idealised positions (244 parameters). Goodness-of-fit = 0.862; $R_1 = 0.0292$ ($I > 2\sigma(I)$), $wR_2 = 0.0616$; min/max residual electron density: $-0.47/0.52$ e Å^{-3}.

5. Supplementary material

Crystallographic data for the structural analysis has been deposited with the Cambridge Crystallographic Data Centre, CCDC no 120568 for compound **4**. Copies of this information may be obtained free of charge from The Director, CCDC, 12 Union Road, Cambridge, CB2 1EZ, UK (Fax: +44-1223-336-033; e-mail: deposit@ccdc.cam.ac.uk or www: http://www.ccdc.cam.ac.uk).

Acknowledgements

We are grateful to the Fonds der Chemischen Industrie (Liebig grant to C.L.), the Deutsche Forschungsgemeinschaft (Habilitandenstipendium), and the Stiftung Volkswagenwerk for financial funding, and especially to Professor J. Daub for his kind support at Regensburg.

References

[1] For a general introduction to non-linear optics of organic compounds, see (a) J.J. Wolff, R. Wortmann, Adv. Phys. Org. Chem. 32 (1999) 121. For organometallic NLO compounds, see (b) I.R. Whittall, A.M. McDonagh, M.G. Humphrey, M. Samoc, Adv. Organomet. Chem. 42 (1998) 2911. (c) N.J. Long, Angew. Chem. 107 (1995) 37.

[2] See e.g. (a) J.C. Calabrese, L.-T. Cheng, J.C. Green, S.R. Marder, W. Tam, J. Am. Chem. Soc. 113 (1991) 7227. (b) D.R. Kanis, M.A. Rantner, T.J. Marks, J. Am. Chem. Soc. 114 (1992) 10338. (c) S.R. Marder, J.W. Perry, B.G. Tiemann, W.P. Schaefer, Organometallics 10 (1991) 1896. (d) U. Behrens, H. Brussaard, U. Hagenau, J. Heck, E. Hendrickx, J. Körmich, J.G.M. van der Linden, A. Persoons, A.L. Spek, N. Veldman, B. Voss, H. Wong, Chem. Eur. J. 2 (1996) 98.

[3] (a) A. Darchen, J. Organomet. Chem. 302 (1986) 389. (b) W.A. Hendrickson, M.C. Palazzotto, Photosensitive metal–organic systems, in: C. Kutal, N. Serpone (Eds.), Advanced Chemistry,

Series 238, ACS, Washington, DC, 1993, pp. 411. (c) D. Astruc, Acc. Chem. Res. 30 (1997) 383.

[4] (a) C. Lambert, S. Stadler, G. Bourhill, C. Bräuchle, Angew. Chem. 108 (1996); Angew. Chem. Int. Ed. Engl. 35 (1996) 644. (b) C. Lambert, E. Schmälzlin, K. Meerholz, C. Bräuchle, Chem. Eur. J. 4 (1998) 512.

[5] M.T. Reetz, G. Lohmer, R. Schwickardi, Angew. Chem. 110 (1998) 492.

[6] A. Le Beuze, R. Lissilour, J. Weber, Organometallics 12 (1993) 47.

[7] For a general introduction to the hyper-Rayleigh scattering technique, see (a) E. Hendrickx, K. Clays, A. Persoons, Acc. Chem. Res. 31 (1998) 675. The experimental set-up used in the present study is described in (b) R. Wortmann, C. Glania, P. Krämer, R. Matschiner, J.J. Wolff, S. Kraft, B. Treptow, E. Barbu, D. Längle, G. Görlitz, Chem. Eur. J. 3 (1997) 1765.

[8] A. Willetts, J.E. Rice, D.M. Burland, D.P. Shelton, J. Chem. Phys. 97 (1992) 7590.

[9] L.-T. Cheng, W. Tam, S.R. Marder, A.E. Stiegman, G. Rikken, C.W. Spengler, J. Phys. Chem. 95 (1991) 10643.

[10] (a) S.R. Marder, L.-T. Cheng, B.G. Tiemann, A.C. Friedli, M. Blanchard-Desce, J.W. Perry, J. Skindhoj, Science 263 (1994) 511. (b) G. Bourhill, J.-L. Bredas, L.-T. Cheng, S.R. Marder, F. Meyers, J.W. Perry, B.G. Tiemann, J. Am. Chem. Soc. 116 (1994) 2619. (c) M. Blanchard-Desce, V. Alain, P.V. Bedworth, S.R. Marder, A. Fort, C. Runser, M. Barzoukas, S. Lebus, R. Wortmann, Chem. Eur. J. 3 (1997) 1091.

[11] C.H. Warren, G. Wettermark, K. Weiss, J. Am. Chem. Soc. 93 (1971) 4658.

[12] I.D.L. Albert, T.J. Marks, M.A. Ratner, J. Phys. Chem. 100 (1996) 9714.

[13] MOS-F V4, Fujitsu Ltd, Japan, 1998. For a general introduction to quantum chemical calculations on NLO properties of organic compounds, see D.R. Kanis, M.A. Ratner, T.J. Marks, Chem. Rev. 94 (1994) 195.

[14] M. Kodomari, H. Satoh, S. Yoshitomi, Bull. Chem. Soc. Jpn. 61 (1988) 4149.

[15] I.U. Khand, P.L. Pauson, W.E. Watts, J. Chem. Soc. C (1968) 2257.

[16] A.E. Tschitschibabin, E.D. Ossetrowa, Chem. Ber. 58 (1925) 1708.